An algorithm for the estimation of the Signal-to-Noise Ratio in surface myoelectric signals generated during cyclic movements

Author's version. Published in: IEEE Trans Biomed Eng. 2012 Jan;59(1):219-25. DOI: 10.1109/TBME.2011.2170687

An Algorithm for the Estimation of the Signal-To-Noise Ratio in Surface Myoelectric Signals Generated During Cyclic Movements

Valentina Agostini and Marco Knaflitz, *Member, IEEE*

***Abstract*—In many applications requiring the study of the surface myoelectric signal (SMES) acquired in dynamic conditions, it is essential to have a quantitative evaluation of the quality of the collected signals. When the activation pattern of a muscle has to be obtained by means of single- or double-threshold statistical detectors, the background noise level (e_{noise}) of the signal is a necessary input parameter. Moreover, the detection strategy of double-threshold detectors may be properly tuned when the signal-to-noise ratio (SNR) and the duty cycle (DC) of the signal are known. The aim of this work is to present an algorithm for the estimation of e_{noise}, SNR and DC of a SMES collected during cyclic movements. The algorithm is validated on synthetic signals with statistical properties similar to those of SMES, as well as on more than a hundred real signals.**

***Index Terms*—Cyclic movements, signal-to-noise ratio (SNR), surface electromyography (sEMG), surface myoelectric signal (SMES).**

I. Introduction

THE analysis of the myoelectric signal allows to determine if a specific muscle is active or silent [1]. Surface myoelectric probes – applied on the skin above the muscle – permit a non-invasive evaluation of the muscle activity.

The traditional use of surface myoelectric signal (SMES) in physiological and biomechanical research [2] was extended to applied research: SMES achieved a well established value as an evaluation tool in surgery planning [3], rehabilitation [4], biofeedback [5]–[6], sports medicine and training [7], and ergonomics research [8].

Among other innovative applications, it is gaining interest the development of advanced human–machine interfaces in which SMES has a key role to play. In particular, myoelectric control [9] is an advanced technique concerned with the detection, processing, classification, and application of SMES to the active control of prosthetic limbs, human-assisting robots, or rehabilitation devices.

The vast majority of the above mentioned applications evaluates muscle activity in dynamic conditions and, in particular, during cyclic or repetitive motor tasks [10]–[12], e.g. walking (gait analysis) [13]–[14] or biking [15]. The movements of the corresponding body segments imply cyclic contractions of muscles. As a consequence, SMES detected from a specific muscle results in a sequence of pseudo-periodical activation bursts [16]. In the time elapsed between the end of a muscle burst and the beginning of the successive one, the muscle under study is silent. However, the probe detects a background noise that is unavoidable in any dynamic test. This background noise is mainly due to crosstalk [2] from neighboring muscles: it is a 'physiological' noise, more relevant than that due to instrumentation.

In order to evaluate the quality of the recorded signals, the background noise and the signal-to-noise ratio are usually estimated by means of manual or automatic segmentation of the signal in the time-domain. To this purpose, myoelectric bursts are separated from muscle baseline activity and the corresponding powers are calculated and compared.

In the analysis of dynamic SMES it is of paramount importance to obtain the onset and offset time instants of a muscle burst, distinguishing the muscle activity from the background noise. The relevance of considering the muscle activation timing is supported by several studies demonstrating its usefulness in orthopedics, treatment of cerebral palsy, and a number of other clinical applications [13].

Well established techniques to determine the activation pattern of a muscle are based on single- or double-threshold statistical detectors [17]–[18]. These detectors require, as a necessary input parameter to set the (first) threshold, the background noise level. Furthermore, double-threshold detectors require additional parameters in order to fine-tune the second threshold. In particular, it is important to estimate the signal-to-noise ratio (SNR) and, to a minor extent, the duty cycle (DC) of the detected signal.

The method we present in this contribution allows to estimate the root-mean-square value of the background noise (e_{noise}), the SNR and the DC of an SMES generated during

*V. Agostini is with the Dipartimento di Elettronica, Politecnico di Torino, 10129 Torino, Italy, (phone: +39-011-5644136; fax: +39-011-5644217; e-mail: valentina.agostini@polito.it).

M. Knaflitz is with the Dipartimento di Elettronica, Politecnico di Torino, 10129 Torino, Italy, (phone: +39-011-5644135; fax: +39-011-5644217; e-mail: marco.knaflitz@polito.it).

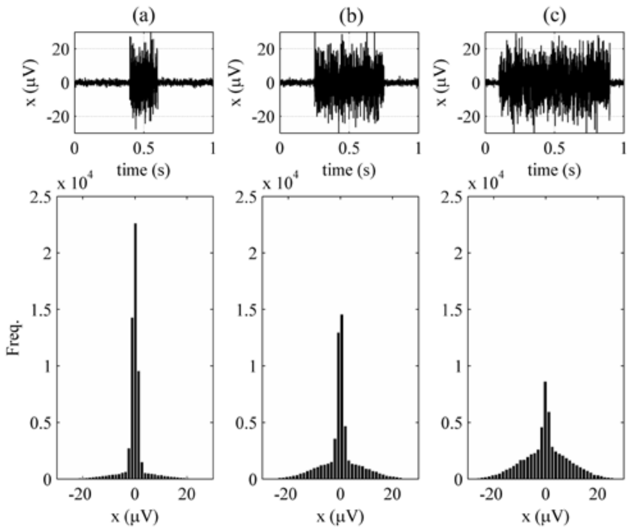

Fig. 1. Cyclo-stationary processes with e_{noise} = 1μV and SNR = 20 dB. Upper plots: representation of a single cycle with (a) DC = 20%, (b) DC = 50%, (c) DC = 80%. Lower plots: histograms of the amplitudes of the three processes. The time support of the signals considered to obtain the histograms is equal to 30 s.

cyclic movements. This is done following a statistical approach that does not require any a priori knowledge on the signal. In this way, we obtain the input parameters necessary to run double-threshold algorithms without the need of pre-processing the signal in the time domain.

II. MATERIALS AND METHODS

A. The surface myoelectric signal in cyclic movements

The SMES recorded during cyclic contractions may be considered as the superposition of the signal generated by the observed muscle during its contraction and the background noise. This noise is mainly due to the activity of neighboring muscles, collected because of the limited spatial selectivity of the detection probe. Moreover, due to the cyclic nature of the movement, this process may be defined as cyclostationary [19]. Its periodicity depends on the cyclic movement under investigation.

In its period of cyclostationarity, the signal can be modeled as the superposition of two stationary processes: noise only, when the muscle is not active, and a second process corresponding to the muscle activity.

When the muscle is non-active (OFF-state) only background noise is present. This noise can be modeled as a Gaussian process with zero-mean and variance σ_n^2:

$$\mathrm{n(t)} \in \mathrm{N}(0, \sigma_n^2) \, . \tag{1}$$

During muscle activity (ON-state), the SMES can be modeled as a zero-mean Gaussian process given by the superimposition of two Gaussian processes corresponding to signal and background noise, respectively:

$$\mathrm{x(t)} = \mathrm{s(t)} + \mathrm{n(t)} \in \mathrm{N}(0, \sigma_s^2 + \sigma_n^2) \, , \tag{2}$$

being σ_s^2 the variance of s(t).

The percentage of time in which the muscle is active with respect to the total cycle duration is referred to as duty cycle.

In the following, it is assumed that the signal x(t) is sampled with a sampling period T_s that satisfies the Nyquist criterion. In particular, since SMES collected by means of usual surface probes typically has more than 99% of the signal power below 500 Hz, we consider a sampling frequency f_c = 2 kHz, that results in a two-time oversampling.

B. Separating signal from noise

The probability density function of the cyclostationary signal considered above is given by the superposition of the probability density functions corresponding to x(t) and n(t) and depends also on the DC. As an example, Fig. 1 reports the histograms of three cyclostationary processes corresponding to e_{noise} equal to 1 μV, SNR equal to 20 dB and DC equal to 20%, 50% and 80%, respectively.

The separation of the ON-state from the OFF-state could be obtained by applying a proper detector, but such detectors would require, as an input parameter, the root-mean-square value of the background noise e_{noise} [18], that is unknown. A possible solution for estimating e_{noise}, without actually separating the ON and OFF states in the time domain, consists of considering an auxiliary time series with a χ^2 distribution. The amplitude histogram of the auxiliary time series has two separated modes, one corresponding to the noise variance and the other to the signal variance.

The auxiliary time series $C_r(k)$ is obtained subdividing the time series x(t) in M epochs constituted by r consecutive samples and then considering the normalized sum of squares of each epoch:

$$C_r(\mathrm{k}) = \sum_{j=1}^{r} \frac{X_{kj}^2}{r} \, , \quad \mathrm{k} = 1,\ldots,\mathrm{M} \, . \tag{3}$$

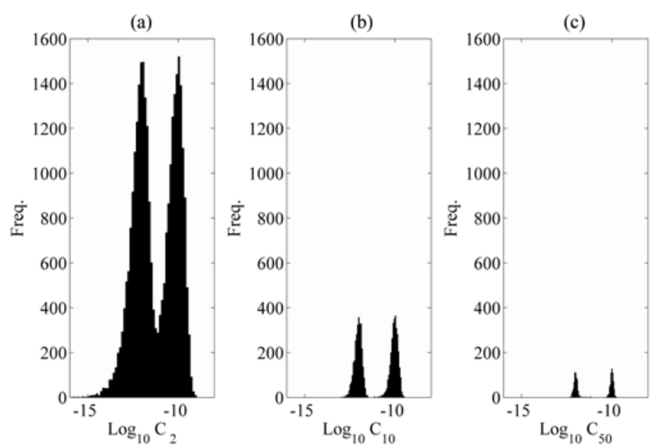

Fig. 2. Histograms of the series of the normalized sum of squares C_r (in logarithmic scale) of a 30s-cyclostationary process with SNR = 20 dB and DC = 50% for (a) r = 2, (b) r = 10, (c) r = 50.

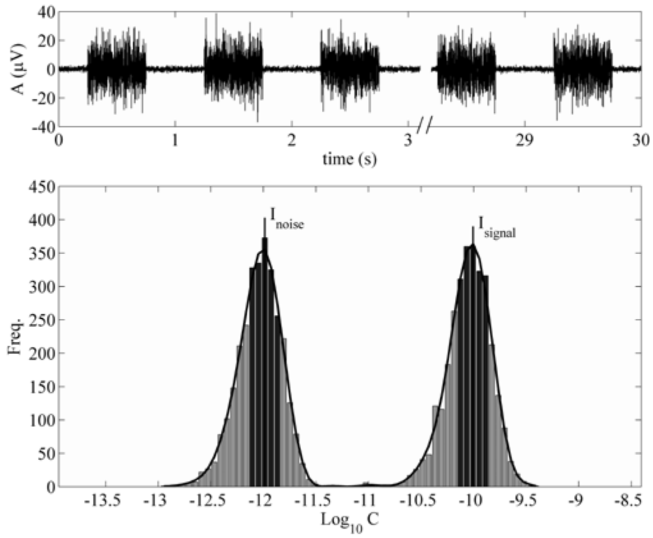

Fig. 3. Histogram of $Log_{10}C$ relative to a cyclic signal with e_{noise} = 1μV, SNR = 20 dB and DC = 50% (time support of the signal = 30 s). The dark-colored bars indicate the bins used by the algorithm to estimate the parameters.

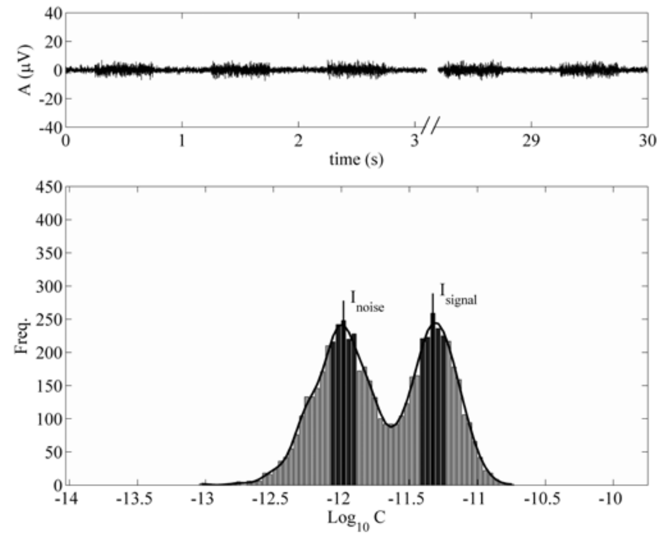

Fig. 4. Histogram of $Log_{10}C$ relative to a cyclic signal with e_{noise} = 1μV, SNR = 6 dB and DC = 50% (time support of the signal = 30 s). The dark-colored bars indicate the bins used by the algorithm to estimate the parameters.

If the signal follows the hypothesized model, the time series has a bimodal distribution with two separated modes. The larger is the difference among σ_n^2 and σ_s^2, the greater is the distance between the modes.

As an example, Fig. 2 reports the bimodal distributions obtained for r = 2, r = 10 and r = 50, respectively. It is evident that increasing r allows for a better separation of the two modes, but contemporarily, due to the reduced size of the series $C_r(k)$, we have a reduced number of samples. Moreover, increasing the r value causes a loss of time resolution from 1 ms (r = 2) up to 25 ms (r = 50). A satisfactory tradeoff may be obtained by choosing r = 10 (time resolution equal to 5 ms). This guarantees an acceptable time resolution, a good separation between the noise and the signal modes, and a sufficient number of samples to build the histogram.

The assumption of gaussianity of the SMES allows to treat the auxiliary time series $C_r(k)$ as χ^2-distributed. This is useful to determine the number of consecutive samples (r) that constitute $C_r(k)$ in an optimal way. However, even if the SMES is not exactly Gaussian, the auxiliary time series will still be two-bell shaped and the algorithm described below will give reliable results.

C. *Description of the algorithm*

In order to estimate e_{noise}, SNR and DC of an SMES generated during cyclic movements we use the following algorithm:

1) Consider the time series $\{x_i\}$, i = 1,…, N, being N the number of samples. In the following, we refer to a time series with a duration equal to 30 s sampled at sampling frequency equal to 2 kHz. It follows that the number of samples N is equal to 60000.

2) Divide $\{x_i\}$ into M = N/r epochs. Considering r = 10 we have:

$$\{X_{kj}\} = \{X_{1j}, X_{2j}, \ldots, X_{Mj}\},\ j = 1, \ldots, 10$$

3) Obtain the auxiliary time series of the normalized sum of squares:

$$C(\mathrm{k}) = \sum_{j=1}^{10} \frac{X_{kj}^2}{10}, \quad \mathrm{k} = 1, \ldots, \mathrm{M}\,. \tag{4}$$

4) Obtain the histogram of the series Log_{10} *C*. The bins of the histogram are defined as:

$$\begin{aligned}\mathrm{bins(m)} \equiv \mathrm{m} \cdot \frac{\max(Log_{10}C) - \min(Log_{10}C)}{2 \cdot Nbins} \\ + \min(Log_{10}C), \quad m = 1,3,...,2 \cdot Nbins - 1.\end{aligned} \tag{5}$$

where Nbins is the number of bins. Since in our case M = 6000, to have a sufficient sample numerosity for each bin we choose Nbins = 60. In general, a number of bins in the range 50-100 is an acceptable choice.

5) Search for local maxima of the curve that interpolates the frequencies of the histogram. Locate the absolute maximum and the highest relative maximum. The leftmost point of maximum is associated to noise (I_{noise}), the rightmost is associated to signal (I_{signal}).

6) Estimate the mean power of the noise, averaging five bins around I_{noise}:

$$P_{\mathrm{noise}} = \frac{\sum_{\mathrm{i}=\mathrm{I_{noise}}-2}^{\mathrm{I_{noise}}+2} \mathrm{bins(i)} \cdot \mathrm{Freq(i)}}{\sum_{\mathrm{i}=\mathrm{I_{noise}}-2}^{\mathrm{I_{noise}}+2} \mathrm{Freq(i)}}\ . \tag{6}$$

7) Estimate the mean power of the signal, averaging five bins around I_{signal}:

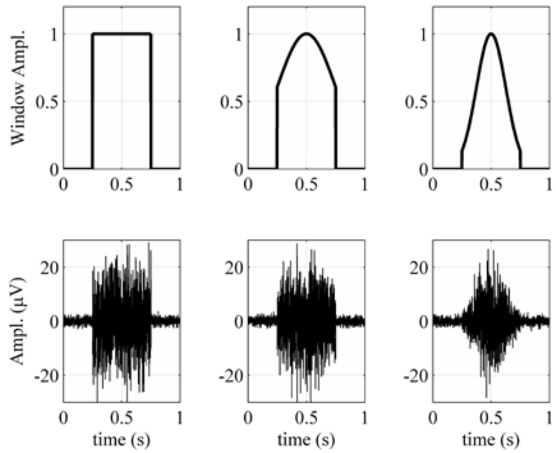

Fig. 5. Representation of 1 cycle of the synthetic SMES obtained with (a) a rectangular window, (b) a Gaussian window with σ=1 and (c) a Gaussian window with σ=2. In this example SNR = 20 dB and DC = 50%.

$$P_{signal} = \frac{\sum_{i=I_{signal}-2}^{I_{signal}+2} \mathrm{bins(i)} \cdot \mathrm{Freq(i)}}{\sum_{i=I_{signal}-2}^{I_{signal}+2} \mathrm{Freq(i)}} . \quad (7)$$

8) Estimate the root-mean-square value of the background noise e_{noise}:

$$e_{noise} = \sqrt{P_{noise}} . \quad (8)$$

9) Estimate the SNR (in dB):

$$SNR = 10 \cdot Log_{10} \frac{P_{signal} - P_{noise}}{P_{noise}} . \quad (9)$$

10) Estimate the duty cycle (%):

$$DC = 100 \cdot \frac{\sum_{i=I_{signal}-2}^{I_{signal}+2} \mathrm{Freq(i)}}{\sum_{i=I_{signal}-2}^{I_{signal}+2} \mathrm{Freq(i)} + \sum_{i=I_{noise}-2}^{I_{noise}+2} \mathrm{Freq(i)}} . \quad (10)$$

In order to clarify how the algorithm works, Fig. 3 represents a 30s-cyclostationary signal with DC = 50% and SNR = 20 dB. Fig. 4 reports a similar example with SNR = 6 dB. As one could have expected, in the 6dB-case there is a partial superposition between the bell-shaped curve relative to the noise and that relative to the signal. However, their modes are still clearly distinguishable.

III. Results and Discussion

A. *Validation of the algorithm*

Synthetic signals are generated with a time duration of 30 s. They are cyclic with a cycle duration of 1 s. They are obtained adding a random process simulating the background noise to a process simulating the SMES generated during a muscle

TABLE I
RECTANGULAR WINDOW

e_{noise} (μV)	20%	40%	60%	80%
6 dB	1.00 ± 0.01	1.00 ± 0.04	1.02 ± 0.03	1.52 ± 0.63
12 dB	1.00 ± 0.01	1.01 ± 0.03	1.00 ± 0.02	1.01 ± 0.04
18 dB	1.00 ± 0.02	1.00 ± 0.02	1.00 ± 0.02	1.00 ± 0.02
24 dB	1.01 ± 0.02	1.00 ± 0.02	1.00 ± 0.02	0.99 ± 0.01
30 dB	0.99 ± 0.02	1.00 ± 0.02	1.00 ± 0.02	1.00 ± 0.03

SNR (dB)	20%	40%	60%	80%
6 dB	5.9 ± 0.3	5.9 ± 0.5	5.7 ± 0.4	3.4 ± 3.0
12 dB	12.0 ± 0.4	11.9 ± 0.4	11.9 ± 0.2	11.9 ± 0.3
18 dB	17.9 ± 0.3	18.1 ± 0.2	17.8 ± 0.2	18.0 ± 0.3
24 dB	23.9 ± 0.2	24.0 ± 0.2	23.9 ± 0.2	24.2 ± 0.2
30 dB	30.0 ± 0.2	30.0 ± 0.2	30.0 ± 0.2	30.0 ± 0.2

DC (%)	20%	40%	60%	80%
6 dB	20.1 ± 0.7	39.6 ± 0.6	59.1 ± 0.6	80.5 ± 6.9
12 dB	19.8 ± 1.0	39.9 ± 0.7	60.2 ± 0.6	80.4 ± 0.6
18 dB	20.2 ± 0.5	40.1 ± 0.6	60.3 ± 0.6	80.3 ± 0.5
24 dB	20.2 ± 0.6	40.4 ± 0.6	60.1 ± 0.7	80.6 ± 0.6
30 dB	20.1 ± 0.4	40.2 ± 0.5	60.4 ± 0.6	80.4 ± 0.3

Estimation of background noise (e_{noise}), signal-to-noise ratio (SNR) and duty cycle (DC) for synthetic signals obtained with a rectangular window. It is reported the mean value estimated over ten realizations ± its standard deviation.

TABLE II
GAUSSIAN WINDOW WITH σ = 1

e_{noise} (μV)	20%	40%	60%	80%
6 dB	0.99 ± 0.03	1.01 ± 0.02	1.17 ± 0.31	1.60 ± 0.47
12 dB	1.00 ± 0.02	1.00 ± 0.02	0.99 ± 0.03	1.00 ± 0.04
18 dB	1.00 ± 0.02	1.00 ± 0.02	1.00 ± 0.02	1.00 ± 0.03
24 dB	1.00 ± 0.02	1.00 ± 0.02	1.00 ± 0.02	1.00 ± 0.03
30 dB	1.00 ± 0.02	0.99 ± 0.02	0.99 ± 0.03	1.00 ± 0.02

SNR (dB)	20%	40%	60%	80%
6 dB	4.5 ± 0.5	4.3 ± 0.6	3.8 ± 1.5	4.1 ± 2.2
12 dB	10.6 ± 0.4	10.6 ± 0.3	10.5 ± 0.5	10.5 ± 0.5
18 dB	16.6 ± 0.4	16.6 ± 0.4	16.5 ± 0.2	16.6 ± 0.5
24 dB	22.5 ± 0.3	22.6 ± 0.3	22.6 ± 0.2	22.6 ± 0.4
30 dB	28.5 ± 0.3	28.6 ± 0.4	28.7 ± 0.2	28.7 ± 0.2

DC (%)	20%	40%	60%	80%
6 dB	18.7 ± 0.7	37.8 ± 5.0	55.1 ± 0.8	71.8 ± 1.5
12 dB	17.7 ± 0.8	36.5 ± 0.5	56.4 ± 0.3	77.7 ± 0.7
18 dB	17.7 ± 0.5	36.1 ± 1.0	56.0 ± 0.7	77.8 ± 0.5
24 dB	17.6 ± 0.3	36.2 ± 0.5	56.1 ± 0.4	77.7 ± 0.4
30 dB	17.8 ± 0.4	36.6 ± 0.6	56.8 ± 0.6	77.7 ± 0.6

Estimation of background noise (e_{noise}), signal-to-noise ratio (SNR) and duty cycle (DC) for synthetic signals obtained with a Gaussian window with σ=1. It is reported the mean value estimated over ten realizations ± its standard deviation.

contraction. Background noise is simulated as a Gaussian process with zero mean and standard deviation equal to 1μV. The SMES burst is generated as a Gaussian process with zero mean and standard deviation equal to $10^{(SNR/20)} \cdot 1\mu V$, windowed on a time support defined by DC. In order to simulate different muscle activation modalities we consider three different types of windows: a) a rectangular window,
b) a Gaussian window with σ=1, c) a Gaussian window with σ=2 (see Fig. 5).

The performances of the algorithm were verified for five different values of the SNR (6, 12, 18, 24, 30 dB) and for four different values of DC (20, 40, 60, 80 %).

TABLE III
GAUSSIAN WINDOW WITH σ = 2

	e_{noise} (μV)			
	20%	40%	60%	80%
6 dB	1.02 ± 0.03	1.05 ± 0.03	1.08 ± 0.04	1.14 ± 0.12
12 dB	1.01 ± 0.02	1.02 ± 0.01	1.05 ± 0.03	1.20 ± 0.33
18 dB	0.99 ± 0.02	1.00 ± 0.02	1.02 ± 0.02	1.49 ± 1.04
24 dB	1.00 ± 0.02	1.00 ± 0.02	1.00 ± 0.03	1.36 ± 1.36
30 dB	1.00 ± 0.02	0.99 ± 0.02	0.99 ± 0.03	1.44 ± 2.19
	SNR (dB)			
	20%	40%	60%	80%
6 dB	4.5 ± 2.5	3.9 ± 2.0	1.2 ± 2.1	0.3 ± 2.1
12 dB	9.2 ± 1.0	9.6 ± 0.6	9.6 ± 0.8	8.2 ± 2.5
18 dB	16.6 ± 0.5	16.3 ± 0.9	16.2 ± 0.5	13.7 ± 4.9
24 dB	21.7 ± 1.0	22.1 ± 0.3	22.4 ± 0.4	21.1 ± 4.5
30 dB	28.2 ± 0.5	28.3 ± 0.5	28.4 ± 0.3	27.4 ± 4.5
	DC (%)			
	20%	40%	60%	80%
6 dB	10.5 ± 1.6	20.9 ± 1.3	36.4 ± 8.1	46.7 ± 9.7
12 dB	10.0 ± 0.4	22.0 ± 0.8	35.6 ± 0.9	50.6 ± 1.2
18 dB	10.0 ± 0.4	22.2 ± 0.8	39.2 ± 0.8	61.3 ± 2.0
24 dB	10.1 ± 0.8	22.9 ± 0.6	39.9 ± 0.9	64.1 ± 1.1
30 dB	10.4 ± 0.4	23.3 ± 0.5	40.8 ± 0.7	64.8 ± 0.8

Estimation of background noise (e_{noise}), signal-to-noise ratio (SNR) and duty cycle (DC) for synthetic signals obtained with a Gaussian window with σ=2. It is reported the mean value estimated over ten realizations ± its standard deviation.

We considered 10 realizations of the described synthetic signals and estimated e_{noise}, SNR and DC for each of them. Then, we calculated the mean value and standard deviation of these parameters over the 10 realizations. Table 1 reports the results relative to the rectangular window, Table 2 those obtained using the Gaussian window with σ = 1, and Table 3 those relative to the Gaussian window with σ = 2.

The estimated background noise (e_{noise}) shows values that are almost always very close to the expected value of 1μV. In the large majority of cases, the corresponding error is lower than 1%. In the rectangular window case (Table 1) the estimated SNR and DC show values that are very close to their expected values. Again, in the large majority of simulation conditions, the error is lower than 1%. In the case of the Gaussian window with σ=1, there is a slight underestimation of SNR and DC (see Table 2). This behavior is reinforced in the case of the Gaussian window with σ=2. In fact, the estimated values are systematically and appreciably lower than the expected ones. This is not surprising and it is due to the shape of the applied window. When dealing with real signals similar to this typology, the estimated values of SNR and DC are always underestimated.

On the contrary, when the Gaussian windows are considered and DC is equal to 80% , the estimated value of the background noise is overestimated up to 60% relative to its true value. The effect of this overestimation is a slight reduction of the sensitivity of the single- or double-threshold detectors, that generally does not compromise their performances.

Although the method herein presented was developed to allow the tuning of statistical detectors, other applications are possible. As an example, the availability of the estimates of e_{noise} and SNR makes it possible to evaluate the quality of the acquired signal in a user independent way. This is of paramount importance to allow for a prompt detection of signals whose quality is not high enough to guarantee reliable results of the processing techniques applied to them.

B. Test of the algorithm on real SMES

Although the validation of the proposed algorithm was carried out working with synthetic SMES, we tested the algorithm also on real signals.

In order to test the applicability of the algorithm to real SMES, recorded during cyclic human movements, we consider - as an example - signals acquired during gait. Our database consists of a total of 142 SMES collected from:

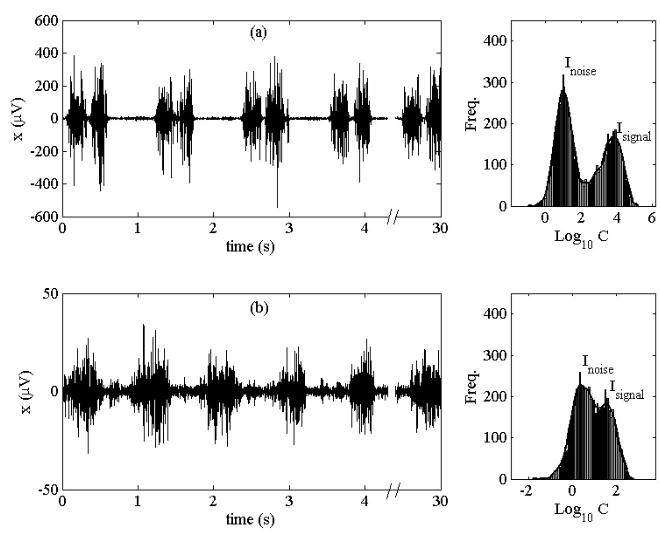

Fig. 6. Examples of application of the algorithm to real signals. (a) SMES from tibialis anterior: enoise1 = 3.2 μV, SNR1 = 28.0 dB, DC1 = 37.8%. (b) SMES from gastrocnemius lateralis: enoise1 = 1.5 μV, SNR1 = 11.3 dB, DC1 = 44.6%.

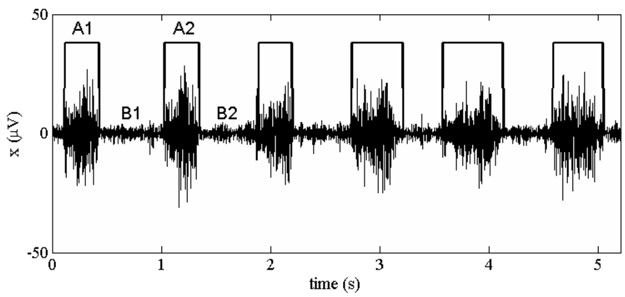

Fig. 7. SMES segmentation in the time domain. The segments labeled as A1, A2, … correspond to muscle activations (= ON states), while B1, B2,… indicate background noise (= OFF states).

tibialis anterior (48), gastrocnemius lateralis (32), lateral hamstrings (24), vastus lateralis (24), rectus femoris (14), The SMES acquisitions were carried out positioning surface myoelectric probes (STEP32, DemItalia, Italy) over the muscle's belly [1]. As for the synthetic signals, we considered a time support of 30 s. The real signals are "pseudo-cyclic" with a cycle duration equal to the subject gait cycle.

Fig. 6 shows an example of SMES collected from (a) tibialis anterior and (b) gastrocnemius lateralis. The corresponding two-bell shaped histograms are shown aside.

We estimated the parameters both with the algorithm described above and by means of an alternative method. The parameters estimated through the proposed algorithm will be indicated as enoise1, SNR1, DC1, while those estimated with the alternative procedure will be indicated as enoise2, SNR2, DC2. The alternative procedure consists of segmenting the 30-s signals in the time domain, obtaining the ON and OFF states by means of the double-threshold detector [18]. An example of signal segmentation is shown in Fig. 7.

Indicating with N the number of segmented gait cycles we define:

$$enoise2 \equiv \frac{1}{\mathrm{N}}\sum_{\mathrm{i=1}}^{\mathrm{N}}\sigma_{\mathrm{Bi}}, \tag{11}$$

where σ_{Bi} is the standard deviation of the i-th background noise segment (see Fig. 7).

Furthermore, we define:

$$S\mathrm{NR2} \equiv 10\cdot\log_{10}\left(\frac{\sigma_{\mathrm{A}}^2}{\sigma_{\mathrm{B}}^2}-1\right), \tag{12}$$

where σ_{A}^2 and σ_{B}^2 are the mean variances of the ON and OFF states, respectively.

Finally, we define:

$$DC2 \equiv \frac{1}{N}\sum_{\mathrm{i=1}}^{\mathrm{N}}\frac{A_i}{A_i+B_i}\cdot 100. \tag{13}$$

Fig. 8 shows the comparison of the two methods on the set of 142 real signals. This figure displays, for each parameter, the scatter plot of the values obtained with the proposed algorithm (x-axis) and with the alternative method (y-axis). To determine how well the proposed algorithm retrieves the values obtained with the "direct" time-domain method we calculated the regression line among the points. The line among enoise1-enoise2 points has a slope close to 1 (0.97) and a very small y-intercept (0.41 μV rms), demonstrating the accuracy of the proposed algorithm in the estimation of background noise. Results are still acceptable when considering the SNR1-SNR2 scatter plot, also if it can be noticed a slight underestimation of SNR1 with respect to SNR2. For what concerns the duty cycle the values obtained with the algorithm are systematically lower than those obtained with the alternative method of about 20% of the gait cycle. These findings are similar to those already commented for the synthetic signals with Gaussian window with σ=1 and, more markedly, in the case σ=2.

IV. Conclusion

This work presents an algorithm for the estimation of background noise, signal-to-noise ratio and duty cycle of SMES generated during cyclic movements. The algorithm was tested on synthetic and real SMES and the obtained results show that, in most practical situations, it provides accurate and stable measures of the aforementioned parameters.

We adopted this method to choose the parameters of a double-threshold statistical detector we previously developed [18] and that we have been using in the past years to carry-out a user independent analysis of the SMES detected during walk. Results we obtained in that field are fully satisfactory and we believe that the approach herein presented could be beneficial also in other applications, when dealing with operator independent processing of SMES or other biomedical

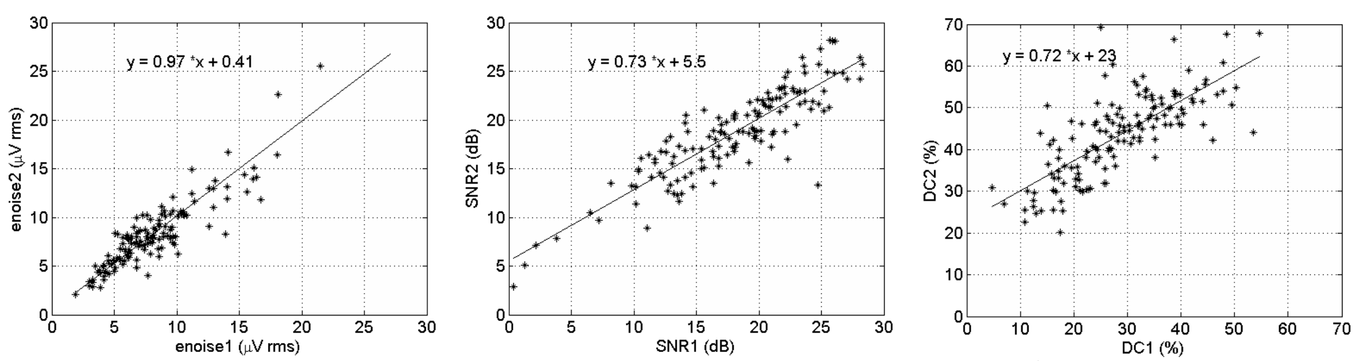

Fig. 8. Scatter plots illustrating the comparison between the two methods. Each point in the plots represents the values of the parameters estimated with: (1) the proposed algorithm (x-axis) and (2) the time-domain method (y-axis), respectively. In each plot the regression line is shown superimposed as well as its corresponding equation.

signals with similar characteristics.

REFERENCES

[1] J. V. Basmajian and C. J. De Luca, *Muscles Alive: Their Functions Revealed by Electromyography*, 5th ed., Williams & Wilkins, Baltimore MD, 1985.

[2] C. J. De Luca, "The Use of Surface Electromyography in Biomechanics", *Journal of Applied Biomechanics*, vol. 13, no. 2, pp. 135–163, 1997.

[3] D. Patikas, S. I. Wolf, W. Schuster, P. Armbrust, T. Dreher, L. Döderlein L. "Electromyographic patterns in children with cerebral palsy: do they change after surgery?", *Gait Posture*, vol. 26, no. 3, pp. 362–71, 2007.

[4] M. G. Benedetti, F. Catani, T. W. Bilotta, M. Marcacci, E. Mariani, S. Giannini, "Muscle activation pattern and gait biomechanics after total knee replacement", *Clin. Biomech.*, vol. 18, pp. 871–876, 2002.

[5] M. A. Crary, M. E. Groher, "Basic Concepts of Surface Electromyographic Biofeedback in the Treatment of Dysphagia", *Am. J. Speech Lang. Pathol.*, vol. 9, pp. 116–125, May 2000.

[6] R. Neblett, Y. Perez, "Surface Electromyography Biofeedback Training to Address Muscle Inhibition as an Adjunct to Postoperative Knee Rehabilitation", *Biofeedback*, vol. 38, no. 2, pp. 56–63, Special Issue, Summer 2010.

[7] R. Zory, F. Molinari, M. Knaflitz, F. Schena, A. Rouard, "Muscle fatigue during cross country sprint assessed by activation patterns and electromyographic signals time–frequency analysis", *Scand. J. Med. Sci. Sports*, doi: 10.1111/j.1600-0838.2010.01124.x, in press, 2010.

[8] G. M. Hägg, A. Luttmann, M. Jäger, "Methodologies for evaluating electromyographic field data in ergonomics, *J. Electromyogr. Kinesiol.*, vol. 10, pp. 301–312, 2000.

[9] M. A. Oskoei, H. Hu, "Myoelectric control systems—A survey", *Biomedical Signal Processing and Control*, vol. 2, pp. 275–294, 2007.

[10] P. Bonato, S. H. Roy, M. Knaflitz, C. J. De Luca, "Time-Frequency Parameters of the Surface Myoelectric Signal for Assessing Muscle Fatigue during Cyclic Dynamic Contractions", *IEEE Trans. Biomed. Eng.*, vol. 48, no. 7, pp. 745–753, 2001.

[11] S. H. Roy, P. Bonato, M. Knaflitz, "EMG assessment of back muscle function during cyclical lifting", *Journal of Electromyography and Kinesiology*, vol. 8, no. 4, pp. 233–245, 1998.

[12] P. Bonato, P. Boissy, U. Della Croce, S. H. Roy, "Changes in the surface EMG signal and the biomechanics of motion during a repetitive lifting task", *IEEE Trans. Neural Syst. Rehabil. Eng.*, vol. 10, pp. 38–47, 2002.

[13] Perry J. *Gait analysis. Normal and pathological function*. Slack Incorporated, Thorofare NJ, 1992.

[14] C. Frigo, P. Crenna, "Multichannel SEMG in clinical gait analysis: a review and state-of-the-art", *Clin. Biomech.*, vol. 24, pp. 236-245, 2009.

[15] M. Knaflitz, F. Molinari, "Assessment of Muscle Fatigue During Biking", *IEEE Trans. Neural Syst. Rehabil. Eng.*, vol. 11, no. 1, pp. 17–23, Mar. 2003.

[16] J.-N. Helal, J. Duchene, "A Pseudoperiodic Model for Myoelectric Signal During Dynamic Exercise", *IEEE Trans. Biomed. Eng.*, vol. 36, no. 11, pp. 1092–1097, 1989.

[17] G. Staude, C. Flachenecker, M. Daumer, W. Wolf, "Onset detection in surface electromyographic signals: a systematic comparison of methods", *EURASIP J. Appl. Signal Process.*, vol. 2, pp. 67–81, 2001.

[18] P. Bonato, T. D'Alessio, M. Knaflitz, "A statistical method for the measurement of muscle activation intervals from surface myoelectric signal during gait", *IEEE Trans. Biomed. Eng.*, vol. 45, pp. 287–299, 1998.

[19] W. A. Gardner, A. Napolitano, L. Paura, "Cyclostationarity: Half a century of research", *Signal Processing*, vol. 86, pp. 639–697, 2006.

Valentina Agostini was born in Rome, Italy, on November 2, 1970. She received the Italian Laurea in physics summa cum laude from the University of Torino, Torino, Italy, in 1995 and the Ph.D. degree in physics from Politecnico di Torino, Torino, Italy, in 2002.

Since 2004 she is with the Dipartimento di Elettronica of Politecnico di Torino, Torino, Italy, as Research Assistant. She focused her research interests in medical imaging and biomedical signal processing since 2004. She worked at the evaluation of the signal-to-noise ratio of infrared image sequences and at the motion artifact reduction in breast dynamic infrared imaging. Her current research interests are in statistical gait analysis and static posturography.

Marco Knaflitz (M'92) was born in Turin, Italy, on January 20, 1955. He received the Italian Laurea in electrical engineering and the Ph.D. in electrical engineering from Politecnico di Torino, Torino, Italy. From 1986 to 1990 he was with the Neuromuscular Research Center of Boston University, Boston, MA, as Research Assistant Professor. From 1995 to 2000 he was appointed Adjunct Professor at the Union Institute of Cincinnati (OH). Since 1990 he has been with the Dipartimento di Elettronica of Politecnico di Torino, Torino, Italy, where he is presently Full Professor of Biomedical Engineering and he teaches Biomedical Instrumentation and Implantable Active Devices.

He has been active since 1985 in the fields of design of biomedical instrumentation and biomedical signal analysis. Specifically, his research interests are mainly focused on the detection and analysis of the myoelectric signal for research and clinical applications.

Prof. Knaflitz is a member of GNB, the Italian national group of bioengineering.